# The first broad-band X-ray study of the Supergiant Fast X-ray Transient SAX J1818.6—1703 in outburst

L. Sidoli, P. Romano, P. Esposito, V. La Parola, J.A. Kennea, H.A. Krimm, M.M. Chester, A. Bazzano, D.N. Burrows, N. Gehrels

- <sup>1</sup>INAF, Istituto di Astrofisica Spaziale e Fisica Cosmica, Via E. Bassini 15, I-20133 Milano, Italy
- <sup>2</sup>INAF, Istituto di Astrofisica Spaziale e Fisica Cosmica, Via U. La Malfa 153, I-90146 Palermo, Italy
- <sup>3</sup>INFN, Sezione di Pavia, Via A. Bassi 6, I-27100, Pavia, Italy
- <sup>4</sup>Department of Astronomy and Astrophysics, Pennsylvania State University, University Park, PA 16802, USA
- $^5$ NASA/Goddard Space Flight Center, Greenbelt, MD 20771, USA
- <sup>6</sup>Universities Space Research Association, Columbia, MD, USA
- <sup>7</sup>INAF, Istituto di Astrofisica Spaziale e Fisica Cosmica, Via Fosso del Cavaliere 100, I-00133, Roma, Italy

#### **ABSTRACT**

The Supergiant Fast X–ray Transient (SFXT) SAX J1818.6–1703 underwent an outburst on 2009 May 6 and was observed with *Swift*. We report on these observations which, for the first time, allow us to study the broad-band spectrum from soft to hard X–rays of this source. No X–ray spectral information was available on this source before the *Swift* monitoring. The spectrum can be deconvolved well with models usually adopted to describe the emission from High Mass X–ray Binary X–ray pulsars, and is characterized by a very high absorption, a flat power law (photon index  $\sim$ 0.1–0.5) and a cutoff at about 7–12 keV. Alternatively, the SAX J1818.6–1703 emission can be described with a Comptonized emission from a cold and optically thick corona, with an electron temperature  $kT_e$ =5–7 keV, a hot seed photon temperature,  $kT_0$ , of 1.3–1.4 keV, and an optical depth for the Comptonizing plasma,  $\tau$ , of about 10. The 1–100 keV luminosity at the peak of the flare is  $3\times10^{36}$  erg s<sup>-1</sup> (assuming the optical counterpart distance of 2.5 kpc). These properties of SAX J1818.6–1703 resemble those of the prototype of the SFXT class, XTE J1739–302. The monitoring with *Swift*/XRT reveals an outburst duration of about 5 days, similarly to other members of the class of SFXTs, confirming SAX J1818.6–1703 as a member of this class.

**Key words:** X-rays: binaries - X-rays: individual (SAX J1818.6–1703)

## 1 INTRODUCTION

Supergiant Fast X-ray Transients (SFXTs) are transient X-ray sources in binary systems composed of a compact object and a blue supergiant companion. Although some of them were discovered before the *INTEGRAL* satellite launch in 2002, this new class of High Mass X-ray Binaries (HMXBs) was recognized only after several new peculiar X-ray transients had been discovered as a result of the Galactic plane survey performed by *INTEGRAL* (Sguera et al. 2005, Negueruela et al. 2006). The members of this new class of sources (about 10, with ~20 candidates) display apparently short outbursts (as observed with *INTEGRAL*), characterized by a few hour duration flares and by a high dynamic range (1,000–100,000) between the quiescence (10<sup>32</sup> erg s<sup>-1</sup>) and the flare peak (10<sup>36</sup>–10<sup>37</sup> erg s<sup>-1</sup>). Spectral properties are very similar to those of High Mass X-ray Binary pulsars (Romano et al. 2008).

Their long-term X–ray properties have been investigated thanks to a monitoring campaign with *Swift* (still ongoing, see Romano et al. 2009b), which is unveiling several new properties of

a sample of SFXTs. This *Swift* campaign has demonstrated that the SFXTs short flares are part of a longer outburst phase lasting days (Sidoli et al. 2009b) and they spend most of their lifetime in accretion at an intermediate level  $(10^{34} \text{ erg s}^{-1})$ , instead of staying in quiescence (as was previously thought; Sidoli et al. 2008). The actual mechanism responsible for the outbursts is still unknown (see Sidoli 2009 for a review of the different proposed scenarios).

SAX J1818.6–1703 is an X–ray source classified as a Supergiant Fast X-ray Transient because of its transient X–ray activity, its high dynamic range (Bozzo et al. 2008) and its association with a blue supergiant star located at 2.5 kpc (O9–B1 type, Negueruela & Smith 2006, Negueruela & Schurch 2007), thanks to the sub-arcsecond X–ray position obtained using *Chandra* (in't Zand et al. 2006). SAX J1818.6–1703 was discovered with the Wide Field Cameras on board *BeppoSAX* (in't Zand et al. 1998), and showed several more bright flares lasting 1–3 hours as observed with IBIS/ISGRI on board *IN-TEGRAL* (Grebenev & Sunyaev 2005, Sguera et al. 2005), reaching ~200 mCrab at the flare peak (18–45 keV), and with ASM

## 2 L. Sidoli et al.

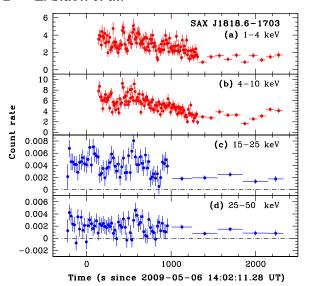


**Figure 1.** XRT and BAT light curves of the 2009 May 6 outburst in units of count  $s^{-1}$  and count  $s^{-1}$  detector<sup>-1</sup>, respectively, showing data collected through the AT observation. The finer sampling points correspond to XRT/WT data (panels a and b) and BAT data in event mode (panels c and d); the remainder are in XRT/PC data and survey mode BAT data.

on board *RXTE* (Sguera et al. 2005). Further and more recent activity has been caught both by *Swift*/BAT (Barthelmy et al. 2008) and by *INTEGRAL* (Grebenev & Sunyaev 2008). A periodicity (likely orbital) of 30-days was discovered (Bird et al. 2009, Zurita Heras & Chaty 2009) from the analysis of available *Swift*/BAT and *INTEGRAL* data, suggesting an eccentric orbit ( $e \sim 0.3-0.4$ ) and an outburst duration of around 4–6 days.

Here we report on the latest outburst from this source, observed with *Swift* starting on 2009 May 6 (Romano et al. 2009d). These *Swift* observations allow us to perform the first broad-band spectroscopy of this SFXT, simultaneously from soft to hard X–rays.

#### 2 OBSERVATIONS AND DATA REDUCTION

SAX J1818.6—1703 triggered the *Swift/*BAT three times since the start of the mission, on 2007 October 16 at 04:20:16 UT (trigger 294385), on 2008 March 15 at 15:54:45 UT (trigger 306379, Barthelmy et al. 2008), and on 2009 May 6 at 14:03:27 UT (trigger 351323, Romano et al. 2009d). In the first two instances *Swift* did not perform a slew, so no narrow-field instrument (NFI) observations are available.

During the flare of 2009 May 6, the subject of this paper, *Swift* executed an immediate slew, so that the XRT began observing the field of SAX J1818.6–1703 about 132 seconds after the BAT trigger. The automated target (AT) observation lasted for one orbit (until approximately 2300 s after the trigger). Follow-up target of opportunity (ToO) observations for 10 ks were obtained by means of a Cycle 5 proposal (PI P. Romano; sequences 00031409001–005, see Table 1) and regular ToO observations (00031409006–010). The data cover the first 14 d since the beginning of the outburst.

The BAT data were analysed using the standard BAT analysis software distributed within FTOOLS. Mask-tagged BAT light curves were created in the standard 4 energy bands, 15–25, 25–50, 50–100, 100–150 keV, and rebinned to achieve a signal-to-noise (S/N)

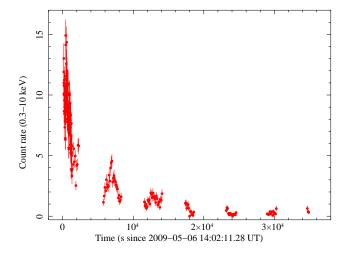


**Figure 2.** *Swift/XRT* light curve of SAX J1818.6—1703 in the energy range 0.3–10 keV, on a linear scale, during the first day of the bright outburst, showing data collected through both AT and GI ToO observations.

of 10 (see Fig. 1c, d). BAT mask-weighted spectra were extracted from event files over the time interval simultaneous with XRT/WT data (see Table 1) and were rebinned to a S/N of 3. Response matrices were generated with BATDRMGEN. For our spectral fitting (XSPEC v11.3.2) we applied an energy-dependent systematic error. Furthermore, survey data products, in the form of Detector Plane Histograms (DPH) with typical integration time of  $\sim 300\,\mathrm{s}$ , are available, and were also analysed with the standard BAT software.

The XRT data were processed with standard procedures (XRTPIPELINE v0.12.1), filtering and screening criteria by using FTOOLS in the HEASOFT package (v.6.6.1). We considered both WT and PC data, selected event grades 0–2 and 0–12, respectively (Burrows et al. 2005). We corrected for pile-up when appropriate by determining the size of the point spread function (PSF) core affected by comparing the observed and nominal PSF (Vaughan et al. 2006; Romano et al. 2006), and excluding from the analysis all the events that fell within that region. To account for the background, we also extracted events within source-free regions. Exposure maps were generated with the task xrtexpomap. Ancillary response files were generated with XRTMKARF, to account for different extraction regions, vignetting, and PSF corrections. We used the spectral redistribution matrices v011 in CALDB.

All quoted uncertainties are given at 90 % confidence level for one interesting parameter unless otherwise stated. The spectral indices are parameterized as  $F_{\nu} \propto \nu^{-\alpha}$ , where  $F_{\nu}$  (erg cm $^{-2}$  s $^{-1}$  Hz $^{-1}$ ) is the flux density as a function of frequency  $\nu$ ; we adopt  $\Gamma = \alpha + 1$  as the photon index,  $N(E) \propto E^{-\Gamma}$  (ph cm $^{-2}$  s $^{-1}$  keV $^{-1}$ ). Times in the light curves and the text are referred to the trigger time.

#### 3 RESULTS

Fig. 1 shows the light curves during the brightest part of the outburst in different energy bands. While the BAT count rate was fairly constant throughout the AT observation, the XRT count rate shows a decreasing trend from a maximum of  $\sim 15~{\rm counts~s^{-1}}$  (in the 0.2–10 keV band, see Fig. 2) with several flares superimposed. The X-ray decreasing trend is even more evident in Fig. 2, which shows the XRT light curve in the 0.3–10 keV band on a linear scale throughout the first day (AT and GI ToO) of observations. The XRT decay

**Table 1.** Summary of the *Swift* observations.

Sequence	Obs/Mode	Start time (UT) (yyyy-mm-dd hh:mm:ss)	End time (UT) (yyyy-mm-dd hh:mm:ss)	Exposure (s)	Time since trigger (s)
00351323000	BAT/event	2009-05-06 13:58:16	2009-05-06 14:18:18	1202	-239
00351323000	BAT/survey	2009-05-06 14:19:03	2009-05-06 14:57:42	1319	1,008
00351323000	XRT/WT	2009-05-06 14:04:32	2009-05-06 14:24:15	1183	138
00351323000	XRT/PC	2009-05-06 14:24:17	2009-05-06 14:40:57	977	1,322
00031409001	XRT/PC	2009-05-06 15:37:42	2009-05-06 23:44:34	9859	5,728
00031409002	XRT/PC	2009-05-07 15:45:00	2009-05-07 18:02:12	4924	92,565
00031409003	XRT/WT	2009-05-08 01:41:00	2009-05-08 17:44:02	168	128, 325
00031409003	XRT/PC	2009-05-08 01:41:11	2009-05-08 17:48:57	4782	128, 336
00031409004	XRT/PC	2009-05-09 03:13:50	2009-05-09 17:46:57	5919	220, 296
00031409005	XRT/PC	2009-05-10 06:30:43	2009-05-10 09:48:41	928	318, 508
00031409006	XRT/PC	2009-05-15 21:43:43	2009-05-15 21:54:58	665	805, 289
00031409007	XRT/PC	2009-05-16 13:30:33	2009-05-16 15:14:57	1083	862, 099
00031409008	XRT/PC	2009-05-17 20:24:37	2009-05-17 22:10:58	1783	973, 343
00031409009	XRT/PC	2009-05-18 15:34:27	2009-05-18 17:13:57	1722	1,042,332
00031409010	XRT/PC	2009-05-19 15:34:28	2009-05-19 17:20:57	1899	1, 128, 734

time during the first day of the outburst can be fitted with an exponential function, with e-folding time,  $\tau_{\rm e}$ , of  $3800\pm100~{\rm s}$ . Note however that this gives only an idea of the general trend, on top of a lot of short term variability.

The XRT spectra of the first six temporal sequences reported in Table 1 have been analysed separately, to search for variability of the spectral parameters along the bright phase of the outburst. The remaining sequences only provided  $3\sigma$  upper limits. In Table 2 we report the spectroscopy results obtained when fitting the spectra with simple models, an absorbed power law or blackbody. More complex deconvolutions of the 1–10 keV spectra are not required by the data. No spectral variability is evident, within the large uncertainties.

We extracted simultaneous BAT and XRT spectra, between 138 and 937 s since the BAT trigger and performed a joint fit in the 1–10 keV and 14–150 keV energy bands for XRT and BAT, respectively. A constant factor was included to allow for normalization uncertainties between the two instruments (always resulted within the usual range). The X–ray spectrum is highly absorbed ( $N_{\rm H}\sim5-7\times10^{22}~{\rm cm}^{-2}$ ) and is very well fit with models we already adopted to describe other SFXTs wide-band spectra (Sidoli et al. 2009a): power laws with high energy cutoffs (CUTOFFPL in XSPEC), or Comptonization models [COMPTT (Titarchuk 1994) or the BMC model (Titarchuk et al. 1996) in XSPEC]. The results of the broadband spectroscopy are summarized in Table 3 (also see Fig. 3).

The BMC model is composed of a blackbody (BB) and its Comptonization and it is not limited to the thermal Comptonization case (COMPTT) but also can account for dynamical (bulk) Comptonization due to the converging flow. The spectral parameters of the BMC model are the black-body (BB) color temperature,  $kT_{\rm BB}$ , the spectral index  $\alpha$  (overall Comptonization efficiency related to an observable quantity in the photon spectrum of the data), and the logarithm of the illuminating factor A,  $\log A$  (an indication of the fraction of the up-scattered BB photons with respect to the BB seed photons directly visible). In SAX J1818.6–1703  $\log A$  could not be constrained and  $\alpha$  was only determined with large uncertainties. Adopting the COMPTT model, the properties of the Comptonizing corona could be constrained well with an an electron temperature  $kT_e{\sim}5{\text -}7$  keV and an optical depth  $\tau{\sim}10$  (in a spherical geometry).

For the timing analysis we only used the XRT observations in which the source was significantly detected. After correcting the photon arrival times to the Solar system barycenter, we extracted the source events with the same selection criteria used for the spectroscopy. We searched each single dataset for coherent sub-orbital pulsations down to a minimum period corresponding to the Nyquist limit (3.532 ms and 5.0146 s for the data collected in WT and in PC modes, respectively) using the  $Z_n^2$  test (Buccheri et al. 1983), with the number of harmonics n being varied from 1 to 4. The period search step size was chosen in each dataset in order to oversample the Fourier period resolution  $(\frac{1}{2}P^2/T_{\rm obs})$  by a factor of 5. No statistically significant signal was detected. The upper limit on the pulsed fraction (defined as the semi-amplitude of the sinusoidal modulation divided by the mean count rate), computed according to Vaughan et al. (1994), is 12 % at the 99 % confidence level and for periods between 3.5 ms and 200 s. In order to search for pulsed signals at long periods (P > 200 s), we analysed together all the data by computing a Lomb-Scargle periodogram (Scargle 1982). Again, we did not detect any significant signal for periods up to  $\sim$ 1000 s, with an upper limit on the pulsed fraction of about 25 % (at the 99 % confidence level).

#### 4 DISCUSSION

SAX J1818.6—1703 is one of the four SFXTs where a period, very likely of orbital origin, has been detected ( $P_{\rm orb}$ ). Such periods have been so far determined either through observations of periodically recurrent outbursts [IGR J11215–5952, Sidoli et al. (2006), Romano et al. (2009c);  $P_{\rm orb} \sim 165$  days] or through a timing analysis of the available hard X–ray data [IGR J18483–0311, Sguera et al. (2007),  $P_{\rm orb} \sim 18.5$  days; IGR J16479–4514, Jain et al. (2009),  $P_{\rm orb} \sim 3.3$  days]. For a fifth SFXT, IGR J08408–4503, we inferred an orbital period of  $\sim 35$  days from the times of the outbursts and the duration of the flares (Romano et al. 2009a).

The SAX J1818.6–1703 orbital period of 30 days has been independently obtained by Bird et al. (2009) and by Zurita Heras & Chaty (2009). Assuming as orbital phase zero the same as Bird et al. (MJD 54540.659), the outburst we analyse here (BAT trigger start time) occurred at orbital phase  $\phi$ =0.90±0.05

## 4 L. Sidoli et al.

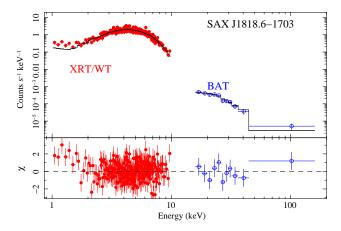


**Figure 3.** Spectroscopy of the 2009 May 6 outburst. **Top:** simultaneous XRT/WT (filled red circles) and BAT (empty blue circles) data fit with an absorbed Comptonization emission (BMC model in XSPEC). **Bottom:** the residuals of the fit (in units of standard deviations).

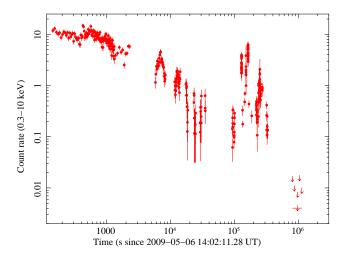


**Figure 4.** *Swift/*XRT light curve of SAX J1818.6—1703 in the energy range 0.3–10 keV, during the whole campaign. The four day gap before the 3  $\sigma$  upper limits is due to the source being Moon constrained. The data shown were collected through both AT and GI ToO, and regular ToO observations.

(1  $\sigma$  error), consistent with the folded light curve and the 4–6 days outburst duration reported by both authors. The new outburst from SAX J1818.6–1703 we are reporting here indeed lasted about 5 days (see Fig. 4), which is also similar to the one in other SFXTs we have been monitoring in the last year with *Swift* (Sidoli et al. 2009a, Romano et al. 2009b) and to the outburst duration in IGR J11215–5952 (Romano et al. 2007).

After the BAT trigger, the whole outburst evolution and the decline phase could be monitored with *Swift*/XRT. The source displays a dynamical range of more than 3000 (see Fig. 4) and a multiple-flaring behaviour previously seen in other SFXTs (Romano et al. 2009a). The temporally resolved spectroscopy with XRT did not result in variability of the spectral parameters in the 1–10 keV range, within the uncertainties, except for the obvious change in the blackbody radius, when fitting the soft X–rays with a single absorbed blackbody (see Table 2). No variability in the absorbing column density could be detected along the outburst, within the uncertainties.

For the first time we obtained broad-band spectroscopy from

soft to hard X-rays of this SFXT, allowing us to compare it with wide-band spectra from a few other SFXTs. Indeed, although SAX J1818.6-1703 has been observed with INTEGRAL (Sguera et al. 2005) in the past, only the high energy part was available (> 20 keV) from the IBIS instrument, and the source spectrum has not been obtained (probably because of the low statistics). The Swift/XRT and BAT joint simultaneous spectrum during the SAX J1818.6–1703 outburst could be fit very well with a cutoff power law (CUTOFFPL in XSPEC) or with Comptonized emission models. It is highly absorbed, shows a flat power law (photon index in the range 0.1-0.5), and displays a cut-off constrained betwen 7 and  $\sim 12$  keV (Table 3). The use of the COMPTT model quantifies the physical conditions of the Comptonizing plasma, resulting in a temperature  $kT_e$  (5-7 keV) for the Comptonizing plasma and the optical depth  $\tau$  of the spherical corona ( $\tau \sim 10$ ). The 1–100 keV luminosity is  $3 \times 10^{36}$  erg s<sup>-1</sup> (assuming 2.5 kpc, Negueruela & Schurch 2007). These SAX J1818.6-1703 broadband properties are reminiscent of the X-ray spectral shape of the prototype of the SFXT class, XTE J1739-302 (Sidoli et al. 2009b, Sidoli et al. 2009a). The two sources indeed display a similarly high absorption, similar X-ray luminosities, energy cutoff values, and hot seed photon temperatures,  $kT_0$ , of 1.3–1.4 keV. These spectral parameters indicate the presence of a cold and optically thick corona, which is also similar to what observed in bright neutron star low mass X-ray binaries (Paizis et al. 2006). No statistically significant pulsations have been found in the Swift/XRT data.

The duration of the outbursts, about 5 days, is also similar to the one observed in other SFXTs we have been monitoring in the last year with *Swift* (Sidoli et al. 2009a, Romano et al. 2009b) and to the outburst duration in IGR J11215–5952 (Romano et al. 2007). All these observed properties, together with the broad-band spectrum we observe now for the first time, confirm the fact that SAX J1818.6–1703 belongs to the class of SFXTs.

#### **ACKNOWLEDGMENTS**

We thank the *Swift* team duty scientists and science planners. We also thank the remainder of the *Swift* XRT and BAT teams, S. Barthelmy in particular, for their invaluable help and support. This work was supported in Italy by contracts ASI I/088/06/0 and I/023/05/0, at PSU by NASA contract NAS5-00136. HAK was supported by the *Swift* project.

#### REFERENCES

Barthelmy, S. D., Krimm, H. A., Markwardt, C. B., Palmer, D. M., & Ukwatta, T. N. 2008, GRB Coordinates Network, 7419, 1 Bird, A. J., Bazzano, A., Hill, A. B., et al. 2009, MNRAS, 393,

Bozzo, E., Campana, S., Stella, L., et al. 2008, Astron. Tel., 1493,

Buccheri, R., Bennett, K., Bignami, G. F., et al. 1983, A&A, 128, 245

Burrows, D. N., Hill, J. E., & Nousek, J. A., et al. 2005, Space Science Reviews, 120, 165

Grebenev, S. A. & Sunyaev, R. A. 2005, Astronomy Letters, 31, 672

Grebenev, S. A. & Sunyaev, R. A. 2008, Astron. Tel., 1482, 1 in 't Zand, J., Heise, J., Smith, M., et al. 1998, IAU Circ., 6840, 2

Table 2. XRT spectroscopy.

Sequence	Power-law $N_{\rm H}$ $(10^{22}~{\rm cm}^{-2})$	Γ	Unabsorbed Flux <sup>a</sup> (1–10 keV)	$\chi^2_{ m red}/dof$ (since trigger)	Times
00351323000 WT 00351323000 PC 00031409001 PC 00031409002 PC 00031409003 WT 00031409003 PC 00031409004 PC 00031409005 PC	$\begin{array}{c} 7.9^{+0.6}_{-0.6} \\ 9.6^{+2.1}_{-1.8} \\ 8.1^{+1.0}_{-0.9} \\ 11.0^{+3.3}_{-2.5} \\ 7.2^{+1.9}_{-1.6} \\ 8.1^{+1.4}_{-1.2} \\ 8.7^{+2.2}_{-1.7} \\ 9.8^{+7.1}_{-1.3} \end{array}$	$\begin{array}{c} 1.1^{+0.1}_{-0.1} \\ 1.1^{+0.4}_{-0.3} \\ 1.7^{+0.2}_{-0.2} \\ 1.9^{+0.6}_{-0.5} \\ 1.9^{+0.5}_{-0.3} \\ 1.5^{+0.3}_{-0.3} \\ 1.4^{+0.4}_{-0.3} \\ 0.9^{+1.6}_{-1.3} \end{array}$	$\begin{array}{c} 1.9^{+0.1}_{-0.1}\times 10^{-9} \\ 1.3^{+0.2}_{-0.1}\times 10^{-9} \\ 3.3^{+0.4}_{-0.1}\times 10^{-10} \\ 5.4^{+2.9}_{-2.0}\times 10^{-11} \\ 9.7^{+0.7}_{-2.0}\times 10^{-10} \\ 2.7^{+0.3}_{-0.3}\times 10^{-10} \\ 1.5^{+0.8}_{-0.8}\times 10^{-11} \\ 5.7^{+0.8}_{-5.7}\times 10^{-11} \end{array}$	1.0/329 1.0/50 0.8/112 0.7/24 0.9/23 0.7/61 0.9/46 0.7/5	138–1, 320 1, 322–2, 299 5, 728–34, 923 92, 565–100, 780 128, 325–186, 108 128, 336–186, 388 220, 296–272, 679 318, 508–330, 367
Sequence	Blackbody $N_{ m H}$ $(10^{22}~{ m cm}^{-2})$	kT (keV)	Unabsorbed Flux <sup>a</sup> (1–10 keV)	$\chi^2_{ m red}/dof$	$R_{ m BB} \  m (km)^b$
00351323000 WT 00351323000 PC 00031409001 PC 00031409002 PC 00031409003 WT 00031409003 PC 00031409004 PC 00031409005 PC	$\begin{array}{c} 4.8^{+0.4}_{-0.4} \\ 4.8^{+0.4}_{-0.4} \\ 6.4^{+1.4}_{-1.2} \\ 4.7^{+0.6}_{-0.5} \\ 6.6^{+2.2}_{-1.7} \\ 4.0^{+1.2}_{-1.0} \\ 4.9^{+0.9}_{-0.8} \\ 5.2^{+1.3}_{-1.1} \\ 6.7^{+3.8}_{-3.8} \end{array}$	$\begin{array}{c} 2.1^{+0.1}_{-0.1} \\ 2.1^{+0.3}_{-0.3} \\ 1.6^{+0.1}_{-0.1} \\ 1.6^{+0.3}_{-0.2} \\ 1.4^{+0.2}_{-0.2} \\ 1.8^{+0.2}_{-0.2} \\ 1.8^{+0.2}_{-0.2} \\ 2.2^{+3.7}_{-0.9} \end{array}$	$\begin{array}{c} 1.4^{+0.1}_{-0.1}\times 10^{-9} \\ 9.3^{+0.2}_{-0.1}\times 10^{-10} \\ 2.0^{+0.1}_{-0.1}\times 10^{-10} \\ 2.3^{+0.8}_{-0.8}\times 10^{-11} \\ 5.2^{+0.3}_{-0.1}\times 10^{-10} \\ 1.7^{+0.3}_{-0.5}\times 10^{-10} \\ 9.7^{+0.3}_{-0.3}\times 10^{-11} \\ 4.2^{+2.4}_{-4.2}\times 10^{-11} \end{array}$	1.0/329 1.0/50 0.8/112 0.7/24 1.0/23 0.9/61 0.8/46 0.8/5	$\begin{array}{c} 0.8^{+0.1}_{-0.1} \\ 0.6^{+0.2}_{-0.1} \\ 0.4^{+0.1}_{-0.1} \\ 0.2^{+0.1}_{-0.1} \\ 0.9^{+0.4}_{-0.2} \\ 0.4^{+0.2}_{-0.2} \\ 0.3^{+0.1}_{-0.1} \\ < 0.3 \end{array}$

<sup>&</sup>lt;sup>a</sup> Fluxes (corrected for the absorption) are in units of erg cm<sup>-2</sup> s<sup>-1</sup>.

**Table 3.** Spectral fits of simultaneous XRT and BAT data of SAX J1818.6—1703.

Model			Parameters					
CUTOFFPL	$N_{\rm H}{}^{\rm a}$ $6.7^{+0.7}_{-0.7}$	$\Gamma$ $0.3^{+0.2}_{-0.2}$	$E_{\text{cut}}^{\text{b}}$ $9.1^{+2.4}_{-1.7}$				Flux <sup>c</sup> 4.8 <sup>+0.1</sup> <sub>-0.1</sub>	$\chi^2_{\nu}$ /d.o.f. 1.0/263
BMC*HIGHECUT	$N_{\rm H}^{\rm a}$ $5.3^{+0.3}_{-0.3}$	$0.3^{+0.2}_{-0.2}$ $kT_{\mathrm{BB}}^{\mathrm{b,d}}$ $1.7^{+0.3}_{-0.3}$	$\alpha^{\text{d}}$ $1.2^{+0.2}_{-1.2}$	$\log(A)^{d}$ 5.7 <sup>+2.3</sup> <sub>-13.7</sub>	$\frac{E_{\rm cut}^{\rm b}}{23_{-8}^{+5}}$	$E_{\text{fold}}^{\text{b}}$ $20_{-14}^{+10}$	Flux <sup>c</sup> 4.2 <sup>+0.1</sup> <sub>-0.1</sub>	$\chi^2_{\nu}$ /d.o.f. 1.0/260
Comptt <sup>e</sup>	$N_{\rm H}^{\rm a}$ $4.5^{+0.6}_{-0.5}$	$kT_0^{\mathrm{b}}$ $1.4^{+0.1}_{-1.0}$	$kT_{e}^{\overline{b}}$ $6.2_{-1.1}^{+0.6}$	$10^{+5}_{-1}$			Flux <sup>c</sup> $4.6^{+0.5}_{-1.8}$	$\chi^2_{ u}$ /d.o.f. $1.0/262$

<sup>&</sup>lt;sup>a</sup> Absorbing column density is in units of  $10^{22}$  cm<sup>-2</sup>.

in't Zand, J., Jonker, P., Mendez, M., & Markwardt, C. 2006, Astron. Tel., 915, 1

Jain, C., Paul, B., & Dutta, A. 2009, MNRAS, in press, arXiv:0903.5403

Negueruela, I. & Schurch, M. P. E. 2007, A&A, 461, 631

Negueruela, I. & Smith, D. M. 2006, Astron. Tel., 831, 1

Negueruela, I., Smith, D. M., Harrison, T. E., & Torrejón, J. M. 2006, ApJ, 638, 982

Paizis, A., et al. 2006, A&A, 459, 187

Romano, P., Campana, S., Chincarini, G., et al. 2006, A&A, 456,

Romano, P., Sidoli, L., Cusumano, G., et al. 2009a, MNRAS, 392, 45

Romano, P., Sidoli, L., Cusumano, G., et al. 2009b, MNRAS, in press, arXiv:0907.1289

Romano, P., Sidoli, L., Cusumano, G., et al. 2009c, ApJ, 696,

Romano, P., Sidoli, L., Krimm, H. A., et al. 2009d, Astron. Tel., 2044, 1

Romano, P., Sidoli, L., Mangano, V., et al. 2008, ApJL, 680, L137 Romano P., Sidoli L., Mangano V., Mereghetti S., Cusumano G., 2007, A&A, 469, L5

Scargle, J. D. 1982, ApJ, 263, 835

Sguera, V., Barlow, E. J., Bird, A. J., et al. 2005, A&A, 444, 221 Sguera, V., Hill, A. B., Bird, A. J., et al. 2007, A&A, 467, 249

Sidoli, L. 2009, Advances in Space Research, 43, 1464

<sup>&</sup>lt;sup>b</sup> Blackbody radii are in units of km, assuming the optical counterpart distance of 2.5 kpc.

 $<sup>^{\</sup>mathrm{b}}$  High energy cutoff ( $E_{\mathrm{cut}}$ ), electron temperature ( $kT_{\mathrm{e}}$ ), seed photons temperature ( $kT_{\mathrm{0}}$ ) and the blackbody color temperature  $kT_{\mathrm{BB}}$  are all in units of keV.

 $<sup>^{\</sup>rm c}$  Unabsorbed 1–100 keV flux is in units of  $10^{-9}$  erg cm $^{-2}$  s $^{-1}$ .

 $<sup>^{</sup>m d}~kT_{
m BB}$  is the blackbody color temperature of the seed photons, lpha is the spectral index and Log(A) is the illumination parameter.

e Assuming a spherical geometry.

## 6 L. Sidoli et al.

Sidoli, L., Paizis, A., & Mereghetti, S. 2006, A&A, 450, L9

Sidoli, L., Romano, P., Ducci, L., et al. 2009a, MNRAS, in press, arXiv:0905.2815

Sidoli, L., Romano, P., Mangano, V., et al. 2009b, ApJ, 690, 120

Sidoli, L., Romano, P., Mangano, V., et al. 2008, ApJ, 687, 1230 Titarchuk, L. 1994, ApJ, 434, 570

Titarchuk, L., Mastichiadis, A., & Kylafis, N. D. 1996, A&AS, 120, C171

Vaughan, B. A., van der Klis, M., Wood, K. S., et al. 1994, ApJ, 435, 362

Vaughan S., Goad M. R., Beardmore A. P., et al., 2006, ApJ, 638, 920

Zurita Heras, J. A. & Chaty, S. 2009, A&A, 493, L1

This paper has been typeset from a  $T_E X / L^A T_E X$  file prepared by the author.